Available online at www.sciencedirect.com
ScienceDirect
Mendeleev Commun., 2015, **25**, 150–152
Mendeleev Communications

Characterization of two Ag^I coordination polymers of the flexible ligand 1,3-bis(4-pyridyl)propane

Min Hu*, Zhuo-Wei Wang, Hui Zhao and Shao-Ming Fang

Zhengzhou University of Light Industry, Henan Provincial Key Laboratory of Surface & Interface Science, Zhengzhou, Henan, 450002 P. R. China. Fax: +86 371 8660 9676; e-mail: humin@zzuli.edu.cn

DOI: 10.1016/j.mencom.2015.03.026

Two new Ag^I coordination polymers having 1-D waved chain and 2-D brick wall structures have been successfully prepared and characterized; the bpp ligands exhibit a rare TT conformation.

The structure of a coordination polymer (CP) depends on both the coordination geometries of metal centers and the coordination behaviors of organic ligands.[1–6] Silver in the oxidation state +1 was found to adopt a wide variety of coordination geometries.[7–9] The fact can be partially contributed to the lack of stereochemical preferences, which arises from a d^{10} configuration. Furthermore, the weakness of silver–ligand bonds supposes that, in the solid state, various weak interactions and crystal packing forces could have greater influence on structure formation than that for more rigid metal–ligand systems.[10] The CPs containing flexible bidentate N-donor ligands are less predictable due to the possible occurrence of supramolecular isomerism involving the adoption of different ligand conformations.[11] 1,3-Bis(4-pyridyl)propane (bpp) can take different conformations (TT, TG, GG and GG′) that display different N-to-N distances by rotating the $(CH_2)_3$ groups.[6,12] However, the use of conformationally flexible ligands may provide unique opportunities to construct novel crystalline architectures with desirable characteristics. In addition, the introduction of a xanthene-9-carboxylic acid (HL) ligand[13,14] bearing a bulky xanthene skeleton as auxiliary ligands into the reaction systems involving flexible ligands, can generate interesting coordination architectures.

To further explore the coordination possibilities of the conformational changes of flexible bidentate ligands with silver metal, we used bpp as a primary ligand to construct photoluminescent Ag^I CPs, and HL auxiliary ligands. Here, we report Ag^I polymers $\{[Ag(bpp)](ClO_4)\}_n$ **1** and $\{[Ag_2(L)(bpp)_2](ClO_4)\cdot MeOH\}_n$ **2**,[†] in which the bpp ligands exhibit a TT conformation.

Single crystal X-ray diffraction analysis[‡] revealed that the crystal structure of **1** consists of 1-D waved cationic chains $\{[Ag(bpp)]^+\}_n$ and perchlorate anions. In the 1-D cationic chain, there is only one unique Ag^I center which adopts a linear geometry coordinated by two pyridyl N-atom donors from two distinct bpp ligands. The Ag–N bond lengths [Ag(1)–N(1), 2.126(5) Å and Ag(1)–N(2#1), 2.128(4) Å, symmetry code: #1 = $-x + 1, -y + 1/2, z - 1/2$] and the N(1)–Ag(1)–N(2#1) angle [173.15(19)°] (see Table S2, Online Supplementary Materials) are within the expected range of such Ag^I complexes [Figure 1(*a*)].[15–17] On the other hand, each μ_2-bridging bpp ligand connects adjacent Ag^I centers to produce a 1-D waved chain along the [001] direction. The TT conformation in **1** leads to an N–to–N separation (9.93 Å) of bpp, which is longer than those in the TG, GG′ and GG conformations associated with this ligand.[11] A further analysis shows that the two pyridyl planes of bpp in **1** are in a rare vertical arrangement. In addition, adjacent 1-D chains were further interlinked by the co-effects of the interchain Ag···O [Ag(1)···O(1), 3.064(3) Å] and C–H···O hydrogen-bonding (see Table S4, Online Supplementary Materials) interactions [C(1)–H(1A)···O(3a), C(9)–

† Elemental analyses were performed on a Vario EL III analyzer. IR spectra were recorded in a range of 400–4000 cm^{-1} on a Tensor 27 OPUS (Bruker) FT-IR spectrometer with KBr pellets.

General procedures for the preparation of complexes **1** *and* **2**.

For **1**: ammonium hydroxide was added dropwise to a methanol solution (5 ml) of bpp (0.1 mmol) and $AgClO_4\cdot 6H_2O$ (0.1 mmol), and the resulting colorless clear solution (pH 12.0) was obtained. Colorless block crystals were formed within a day. Yield ~40% on a bpp basis. IR (KBr pellet, ν/cm^{-1}): 3061 (w), 2941 (w), 1617 (s), 1558 (m), 1507 (m), 1468 (m), 1432 (s), 1347 (w), 1238 (m), 1087 (vs), 862 (m), 823 (m), 803 (m), 747 (w), 620 (s), 584 (w), 520 (m), 484 (w). Found (%): C, 38.48; H, 2.69; N, 6.81. Calc. for $C_{13}H_{11}AgClN_2O_4$ (%): C, 38.91; H, 2.76; N, 6.99.

For **2**: the pH value of a methanol solution (5 ml) of HL (0.1 mmol) and bpp (0.1 mmol) was adjusted to 12.0 by adding ammonium hydroxide, and then it was mixed with an aqueous solution (5 ml) of $AgClO_4\cdot 6H_2O$ (0.1 mmol). After several days, yellow block single crystals were obtained. Yield ~35% on a bpp basis. IR (KBr pellet, ν/cm^{-1}): 3363 (br. m), 1602 (s), 1585 (s), 1501 (w), 1481 (s), 1454 (m), 1432 (m), 1353 (m), 1301 (w), 1257 (s), 1223 (m), 1087 (vs), 1028 (m), 912 (w), 853 (w), 812 (m), 768 (m), 689 (w), 621 (m), 517 (m). Found (%): C, 50.62; H, 4.45; N, 5.64. Calc. for $C_{41}H_{41}Ag_2ClN_4O_8$ (%): C, 50.82; H, 4.26; N, 5.78.

‡ Single-crystal X-ray diffraction measurements were carried out on a Bruker Smart 1000 CCD diffractometer equipped with a graphite crystal monochromator situated in the incident beam for data collection at 294(2) K. The determinations of unit cell parameters and data collections were performed with MoKα radiation (λ = 0.71073 Å), and unit cell dimensions were obtained with least-squares refinements. The SAINT program was used for the integration of diffraction profiles. Semi-empirical absorption corrections were applied using the SADABS program. All the structures were solved by direct methods using the SHELXS program of the SHELXTL package and refined by full-matrix least-squares methods with SHELXL (semi-empirical absorption corrections were applied using SADABS program). Ag^I atoms in each complex were located from the *E*-maps and the other non-hydrogen atoms were located in successive difference Fourier syntheses and refined with anisotropic thermal parameters on F^2 values.[18] The hydrogen atoms were added theoretically, riding on the concerned atoms and refined with fixed thermal factors.

Selected crystallographic data for $C_{13}H_{11}AgClN_2O_4$ **1**. Orthorhombic, space group *Cmca*, a = 7.1013(8), b = 15.0391(9) and c = 27.3815(18) Å, V = 2924.3(4) $Å^3$, Z = 8, d_{calc} = 1.829 g cm^{-3}; μ = 1.577 mm^{-1}; data/restraints/parameters 1399/0/127; S = 1.004. Final R indices [$I > 2\sigma(I)$]: R_1 = 0.0311, wR_2 = 0.0371. R indices (all data): R_1 = 0.0872, wR_2 = 0.0396.

Selected crystallographic data for $C_{41}H_{41}Ag_2ClN_4O_8$ **2**. Orthorhombic, space group *Pbca*, a = 17.7597(12), b = 18.1136(10) and c = 25.4503(11) Å, V = 8187.2(8) $Å^3$, Z = 8, d_{calc} = 1.572 g cm^{-3}; μ = 1.078 mm^{-1}; data/restraints/parameters: 7196/0/507; S = 1.065. Final R indices [$I > 2\sigma(I)$]: R_1 = 0.0371, wR_2 = 0.0419. R indices (all data): R_1 = 0.1078, wR_2 = 0.0438.

CCDC 811810 and 1008400 contain the supplementary crystallographic data for this paper. These data can be obtained free of charge from The Cambridge Crystallographic Data Centre *via* http://www.ccdc.cam.ac.uk.

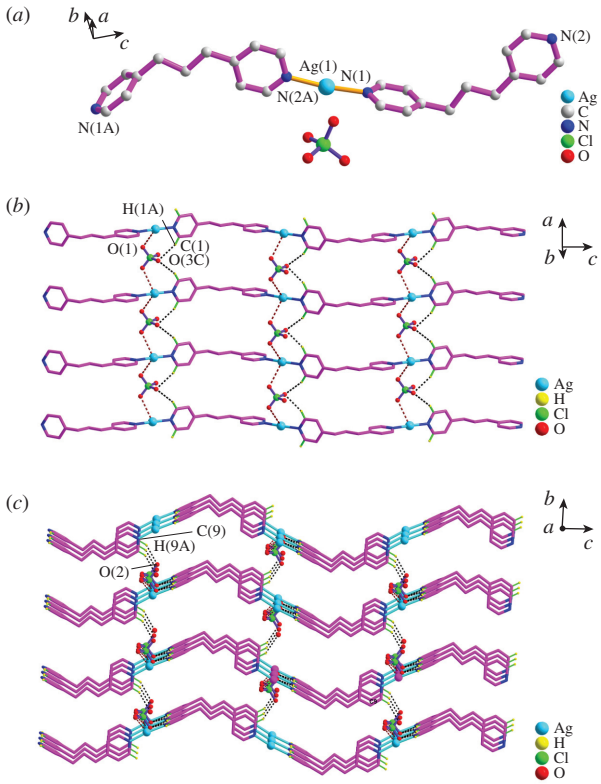

Figure 1 (*a*) Coordination environment of Ag^{I} in **1**, (*b*) the 2-D layered network running parallel to the (010) plane, and (*c*) the 3-D supramolecular framework formed by the intermolecular C–H···O hydrogen bonds (dashed lines). Only H atoms involved in the interactions are shown for clarity. The symmetry-related atoms labeled with the suffixes A are generated by the symmetry operation ($-x + 1$, $-y + 1/2$, $z - 1/2$).

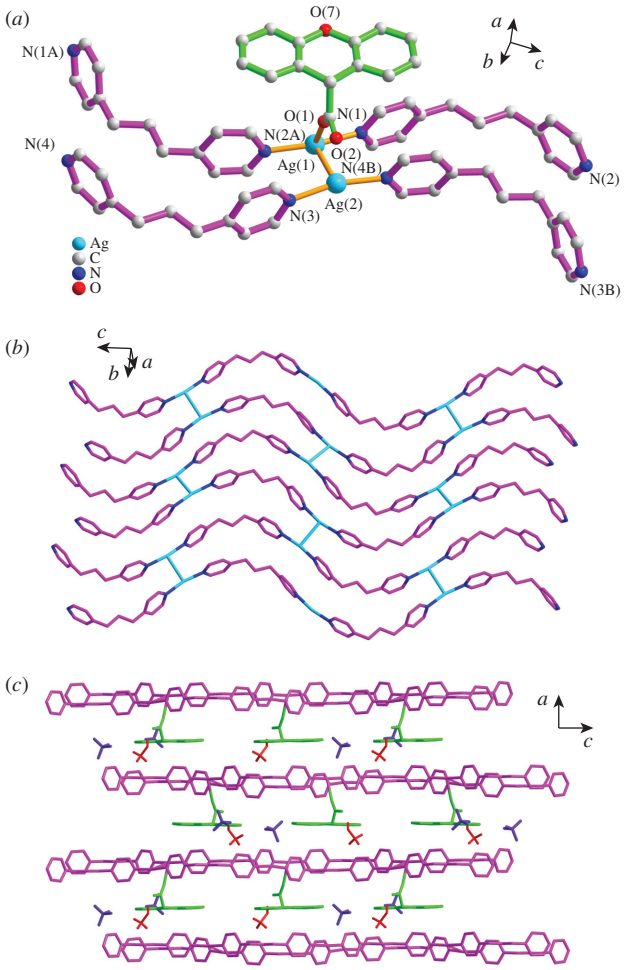

Figure 2 (*a*) Coordination environment of Ag^{I} in **2**; (*b*) 2-D $[Ag_2(bpp)_2]_n^{2n+}$ wavelike brick wall structure in **2**, silver atoms and Ag–Ag bonds are in turquoise, L ligands are omitted for clarity; (*c*) the sandwich-like network constructed with 2-D $[Ag_2(bpp)_2(L)]_n^{n+}$ layers, ClO_4^- anions and MeOH molecules. Partial L ligands are omitted for clarity. The symmetry-related atoms labeled with the suffixes A and B are generated by the symmetry operation (x, $-y + 1/2$, $z - 1/2$) and ($-x + 3/2$, $-y$, $z + 1/2$).

H(9A)···O(2b); symmetry codes: $a = x - 1/2$, y, $-z + 1/2$; $b = x$, $-y$, $-z + 1$; Table S3] between ClO_4^- and pyridyl rings of bpp to form a 2-D layered network running parallel to the (010) plane [Figure 1(*b*)], and then an overall 3-D supramolecular framework [Figure 1(*c*)].

One carboxylate ligand L bearing a bulky xanthene skeleton was chosen to investigate its effects on the Ag^{I} system; 2-D layers structure was isolated. Each asymmetric unit contains two crystallographically unique silver sites [Ag(1) and Ag(2)] [Figure 2(*a*)], two bpp ligands, one coordinated L anion, one free perchlorate anion and one guest methanol molecule. The Ag(1) has the T-shaped coordination geometry surrounded by two nitrogen atoms from two distinct bpp ligands and one weakly coordinated carboxylate group from L ligand [Ag(1)–N(1), 2.148(3), Ag(1)–N(2), 2.148(3) and Ag(1)–O(1), 2.560(4) Å] (see Table S3). As for Ag(2), it is in a linear geometry coordinated by two nitrogen atoms from separate bpp ligands [Ag(2)–N(2), 2.170(3) and Ag(2)–N(3), 2.170(3) Å]. The Ag(1) and Ag(2) atoms are ligated to form a binuclear silver unit by a close Ag–Ag contact [Ag(1)–Ag(2), 3.006(4) Å]. The intramolecular Ag–Ag separation is shorter than the sum of the van der Waals radii of two silver atoms (3.44 Å),[19,20] which indicates relatively strong intramolecular argentophilicity in **2**. The carboxylate of L ligand binds to Ag(1) through μ_1-η^1:η^0-monodentate mode. The bpp ligands display the TT conformation [N(1)-to-N(2), 9.58 Å and N(3)-to-N(4), 9.50 Å], but the two pyridyl planes of bpp in **2** are not in the vertical arrangement; the dihedral angles are 70.28° [the N(1)/N(2) pyridyl planes] and 72.89° [the N(3)/N(4) pyridyl planes], respectively. Compared to complex **1**, the steric bulk of xanthene skeleton of carboxylate ligand L may play an important role in the adoption of bpp ligand conformations. Furthermore, each μ_2-bridging bpp ligand connects two binuclear silver units and complex **2** can be extended into a 2-D framework. Topologically, this 2-D network could be pictured as a wavelike brick wall [Figure 2(*b*)]. Furthermore, the perchlorate anions are intercalated between the parallel layers and involved in second-sphere interactions; the adjacent 2-D layers are further assembled to form a sandwich-like 3-D supramolecular network running along the [010] plain [Figure 2(*c*)] by the inter-layer Ag···O interactions [Ag(2)···O(3), 2.967(7) Å] and C–H···O hydrogen-bonding interactions (see Table S4) between perchlorate anions and the bpp ligands of adjacent 2-D layers.

To confirm whether the crystal structures are truly representative of the bulk materials, X-ray powder diffraction experiments have also been carried out for **1** and **2** (see Figure S1). The experimental patterns can be considered favorably that the synthesized bulk materials and the as-grown crystals are homogeneous for **1** and **2**.

Complexes **1** and **2** are stable under ambient conditions, and thermogravimetric experiments were performed to explore their thermal stabilities. The TGA curves of **1** and **2** (see Figure S2) are different, probably, due to their different architectures. For **1**, the first weight loss of 26.20% occurs from 130 to 310 °C (peaking at 271 °C), which is attributed to the loss of free ClO_4^- anions (calc. 24.52%). Then, the host structure starts to decompose quickly and it does not stop until heating ends at 900 °C. With regard to **2**, lattice methanol guests (calc. 3.31%) and free ClO_4^- anions (calc. 10.26%) are released from 30 to 184 °C (peaking at 111 and 173 °C), as revealed by a total weight loss of

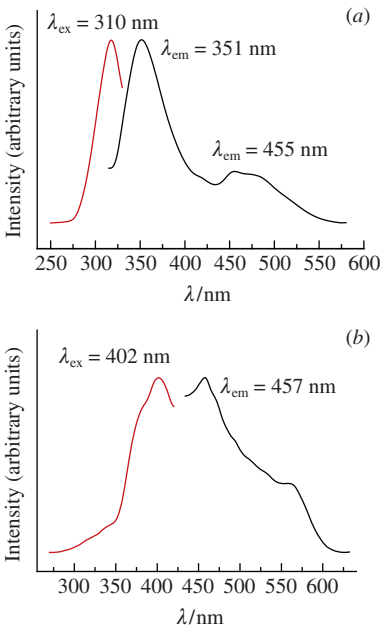

Figure 3 Excitation/emission spectra of complexes (*a*) **1** and (*b*) **2** at room temperature.

13.84%. With that, the decomposition of the residuary components occurs with one sharp weight decrease (peaking at 275 °C), which can be attributed to the loss of L and part bpp ligands, showing the collapse of the 2-D coordination framework.

The synthesis of luminescent coordination complexes with selected ligands and d^{10} metal centers is an efficient method for producing new luminescence materials.[21,19] The solid-state emission spectra of complexes **1** and **2** were investigated at room temperature (Figure 3). The free bpp ligand shows a maximal emission peak at 463 nm (λ_{ex} = 373 nm), which can be ascribed to the $\pi \rightarrow \pi^*$ and/or $n \rightarrow \pi^*$ transitions. To further analyze the nature of these emission bands, the photoluminescent properties of HL were studied under the same experimental conditions (λ_{max} = 474 nm, λ_{ex} = 426 nm). Excitation of the microcrystalline sample of **1** at 310 nm produces two emission peaks at λ_{max} of 351 and 455 nm. We assume that the emission peak at 351 nm can be assigned to ligand to metal charge-transfer (LMCT) transition,[22] and the peak at 455 nm corresponds to the emission spectra of ligand to ligand charge-transfer (LLCT) transition of bpp. As for complex **2**, comparing with the emission peak of HL ligand at 474 nm, the emission peaks at 457 nm can be tentatively assigned to intraligand transfer $\pi^* \rightarrow \pi$ transitions.

In conclusion, we have successfully constructed two photoluminescent Ag^{I} CPs, in which the bpp ligands exhibit a TT conformation. The structural difference of complexes **1** and **2** can be attributed to the introduction of a carboxylate ligand bearing a bulky xanthene skeleton. The procedure described here can be generally used to react with different transition metal ions for constructing other coordination complexes with fascinating structures and potential properties.

This work was supported by the National Natural Science Foundation of China (grant no. 21171151).

Online Supplementary Materials

Supplementary data associated with this article can be found in the online version at doi:10.1016/j.mencom.2015.03.026.

References

1 M. Du, C.-P. Li, C.-S. Liu and S.-M. Fang, *Coord. Chem. Rev.*, 2013, **257**, 1282.
2 F. Jin, Y. Zhang, H.-Z. Wang, H.-Z. Zhu, Y. Yan, J. Zhang, J.-Y. Wu, Y.-P. Tian and H.-P. Zhou, *Cryst. Growth Des.*, 2013, **13**, 1978.
3 V. Madhu and S. K. Das, *Cryst. Growth Des.*, 2014, **14**, 2343.
4 Z. Zhang and M. J. Zaworotko, *Chem. Soc. Rev.*, 2014, **43**, 5444.
5 P.-C. Cheng, C.-W. Yeh, W. Hsu, T.-R. Chen, H.-W. Wang, J.-D. Chen and J.-C. Wang, *Cryst. Growth Des.*, 2012, **12**, 943.
6 J.-S. Hu, X.-M. Zhang, H.-L. Xing, J. He and J.-J. Shi, *Mendeleev Commun.*, 2013, **23**, 231.
7 H.-Y. Shi, Y.-B. Dong, Y.-Y. Liu and J.-F. Ma, *CrystEngComm*, 2014, **16**, 5110.
8 X.-Y. Qian, J.-L. Song and J.-G. Mao, *Inorg. Chem.*, 2013, **52**, 1843.
9 K. M. Patil, S. A. Cameron, S. C. Moratti and L. R. Hanton, *CrystEngComm*, 2014, **16**, 4587.
10 L. Cunha-Silva, M. J. Carr, J. D. Kennedy and M. J. Hardie, *Cryst. Growth Des.*, 2013, **13**, 3162.
11 F. C. Pigge, *CrystEngComm*, 2011, **13**, 1733.
12 L. Carlucci, G. Ciani, D. M. Proserpio and S. Rizzato, *CrystEngComm*, 2002, **4**, 121.
13 L.-R. Jia, M. Hu, S.-M. Fang and C.-S. Liu, *J. Coord. Chem.*, 2011, **64**, 1849.
14 R. Shyni, S. Biju, M. L. P. Reddy, A. H. Cowley and M. Findlater, *Inorg. Chem.*, 2007, **46**, 11025.
15 G.-G. Luo, D.-L. Wu, L. Liu, J.-X. Xia, D.-X. Li, C. Peng, Z.-J. Xiao and J.-C. Dai, *Inorg. Chem. Commun.*, 2012, **15**, 272.
16 M.-L. Tong, Y.-M. Wu, J. Ru, X.-M. Chen, H.-C. Chang and S. Kitagawa, *Inorg. Chem.*, 2001, **41**, 4846.
17 G.-P. Yang, Y.-Y. Wang, P. Liu, A.-Y. Fu, Y.-N. Zhang, J.-C. Jin and Q.-Z. Shi, *Cryst. Growth Des.*, 2010, **10**, 1443.
18 *Bruker 2000, SMART (Version 5.0), SAINT-plus (Version 6), SHELXTL (Version 6.1), SADABS (Version 2.03)*, Bruker AXS Inc., Madison, WI.
19 J.-C. Jin, Y.-Y. Wang, W.-H. Zhang, A. S. Lermontov, E. K. Lermontova and Q.-Z. Shi, *Dalton Trans.*, 2009, 10181.
20 P.-X. Yin, J. Zhang, Z.-J. Li, Y.-Y. Qin, J.-K. Cheng, L. Zhang, Q.-P. Lin and Y.-G. Yao, *Cryst. Growth Des.*, 2009, **9**, 4884.
21 P. Horcajada, R. Gref, T. Baati, P. K. Allan, G. Maurin, G. Couvreur, P. Férey, R. E. Morris and C. Serre, *Chem. Pap.*, 2011, **112**, 1232.
22 D. Sun, N. Zhang, R.-B. Huang and L.-S. Zheng, *Cryst. Growth Des.*, 2010, **10**, 3699.

Received: 4th July 2014; Com. 14/4415